Automatica 151 (2023) 110902

Contents lists available at ScienceDirect

Automatica

journal homepage: www.elsevier.com/locate/automatica

Brief paper

Chattering-free adaptive iterative learning for attitude tracking control of uncertain spacecraft☆

Fan Zhang [a,b], Deyuan Meng [a,b,*], Xuefang Li [c]

[a] The Seventh Research Division, Beihang University (BUAA), Beijing 100191, PR China
[b] School of Automation Science and Electrical Engineering, Beihang University (BUAA), Beijing 100191, PR China
[c] School of Intelligent Systems Engineering, Sun Yat-Sen University, Guangzhou 510275, PR China

ARTICLE INFO

Article history:
Received 17 November 2021
Received in revised form 30 September 2022
Accepted 25 December 2022
Available online 24 February 2023

Keywords:
Adaptive iterative learning
Attitude tracking
Chattering free control
Initial state error
Reduction mechanism
Spacecraft

ABSTRACT

This paper aims at developing chattering-free adaptive iterative learning for repetitive attitude tracking tasks of spacecraft subject to initial state errors. Thanks to the proposed reduction mechanism in the parametric learning law, iteration-varying initial state errors, as well as the unknown inertia matrix and external disturbances, can be addressed effectively. Moreover, to avoid the chattering phenomenon of the control signals, we introduce an approximation of the sign function. Of note is that this approximation leads to a class of non-negative definite problems. A new analytical method is consequently exploited with a Lyapunov-like theory based on contraction-mapping and composite-energy-function, which rigorously shows the boundedness and convergence of the iterative learning process in the presence of initial state errors and non-negative definite problems. These observations are validated by implementing the proposed chattering-free adaptive iterative learning method to achieve the specific attitude tracking task of an uncertain spacecraft.

1. Introduction

Attitude tracking control is required for many applications of spacecraft (Cavalcanti, Figueredo, & Ishihara, 2018; Hu, Xiao, Wang, & Poh, 2013; Petersen, Leve, & Kolmanovsky, 2017; Riel, Sinn, Schwaer, Ploner, & Schitter, 2019; Zhao & Duan, 2021). To improve the robustness and tracking precision, various feedback methods has been exploited, such as sliding mode control (Hu et al., 2013), model predictive control (Petersen et al., 2017), adaptive control (Zhao & Duan, 2021), optimal control (Cavalcanti et al., 2018). It is worth noticing that most of the above methods mainly focus on the steady state performance of systems. For some specific scenarios, such as spacecraft-based remote observations (Lang & de Ruiter, 2022) and the power transmission through laser (Li, Deng, Zhang, & Wang, 2018), the transient performance of the attitude tracking tasks is also critically important. Specifically, A spacecraft is required to robustly and exactly track some predefined attitude trajectory over a time duration periodically, such that the on-board payloads, e.g., cameras or transmitting antennas, could accurately point to the specific target (Li, Wei, Deng, Wu, & Jiang, 2021). For such kinds of finite-time perfect tracking objectives, it is difficult to implement conventional feedback control methods (Riel et al., 2019), especially when initial state errors exist.

Iterative learning control (ILC), categorized as one of the intelligent control algorithms, usually focuses on achieving the perfect tracking instead of the asymptotic tracking over a fixed duration (see Bristow, Tharayil, & Alleyne, 2006 and references therein for more explanations). By learning from historical data, ILC can gradually refine the tracking performance along the iteration axis (Altın & Barton, 2017; Tayebi, Abdul, Zaremba, & Ye, 2008). Generally, the implementation of the conventional ILC requires an assumption upon the strict repetitiveness of the system (Cobb et al., 2022; Zhang & Meng, 2022), which may not be satisfied for the attitude tracking tasks due to iteration-varying uncertainties and the non-identical initial condition. In literature, some robust ILC methods have been developed to handle non-repetitive system uncertainties and external disturbances under the frameworks of contraction-mapping (CM) (Lee, Rai, & Tsao, 2022; Sammons, Hoelzle, & Barton, 2020; Zhang & Meng, 2021, 2022) and composite-energy-function (CEF) (Jin, 2019; Li, Huang,

☆ This work was supported in part by the National Natural Science Foundation of China under Grant 62273018, Grant 61922007, and Grant 62003376, and in part by the Science and Technology on Space Intelligent Control Laboratory under Grant HTKJ2022KL502006. The material in this paper was not presented at any conference. This paper was recommended for publication in revised form by Associate Editor Abdelhamid Tayebi under the direction of Editor Thomas Parisini.

* Corresponding author at: The Seventh Research Division, Beihang University (BUAA), Beijing 100191, PR China.
E-mail addresses: zhangfan_buaa@buaa.edu.cn (F. Zhang), dymeng@buaa.edu.cn (D. Meng), lixuef25@mail.sysu.edu.cn (X. Li).

https://doi.org/10.1016/j.automatica.2023.110902
0005-1098/

Chu, & Xu, 2016; Tayebi, 2004). However, some issues, such as CEF-based adaptive ILC with both iteration-varying initial state errors and system uncertainties, are still challenging in the design and analysis.

Recently, several works related to adaptive ILC have been reported on handling initial state errors under the framework of CEF. Most of the works rely on a rectifying action within an initial time interval, at the end of which the state errors are required to be zero (see, e.g., Yang, Xu, Huang, and Tan (2015) and Jin (2017)). This is hard to implement when initial state errors are sufficiently small due to the hardware limit of the servo-mechanisms. The boundary layer strategies are also exploited to enhance the robustness of adaptive ILC against initial state errors in Chien (2008), Xie and Sun (2009), and Yin, Xu, and Hou (2011). But it is difficult to apply this method directly to the attitude tracking control systems, since the derivative of the boundary layer function does not exist for systems with multiple degree-of-freedom. A deadzone mechanism is developed to address initial state errors with known uniform bounds in Zhang, Meng, and Li (2022), which involves the known inertia matrix. This motivates us to improve the robustness of conventional adaptive ILC against initial state errors in the case of little model knowledge.

In addition, the chattering phenomenon of control signals is also considered to be one of the important issues for the applications of adaptive ILC. This is mainly because the chattering phenomenon easily excites the high-frequency unmodeled dynamics and thus degrades the control performance (Li et al., 2016). This problem could not be addressed well in the field of conventional adaptive ILC. The reason is that CEF-based adaptive ILC depends heavily on the sign function, which is employed to guarantee the monotonicity and boundedness of CEF. To exclude the chattering phenomenon, the continuous approximations of the sign function should be presented. In such a case, it is challenging to tackle the non-negative definite problem arising from the controller without sign switching and to guarantee the boundedness and the convergence of CEF.

Inspired by the idea in Tayebi (2004), we provide new insights into CEF-based adaptive ILC by proposing a robust adaptive ILC method equipped with a reduction mechanism, smoothing the control input by the hyperbolic tangent function, and implementing the robustness analysis against initial state errors as well as other uncertainties. With the proposed control strategy, the attitude tracking problem of spacecraft can be addressed effectively, and thus the application scope of adaptive ILC can be further expanded. Through comparisons with existing results of adaptive ILC, the main contributions are highlighted succinctly as follows.

(1) For the periodic attitude tracking tasks with multiple degrees of freedom, we develop a novel adaptive ILC scheme, which practically smooths the inputs and simultaneously enhances the robustness against the completely unknown inertia matrix, iteration-varying initial state errors, and external disturbances. Compared with existing adaptive ILC in Wu, Wang, and Poh (2015) and Lang and de Ruiter (2022), the design of the proposed method does not require the prior information of the inertia matrix, the uniform bounds of initial state errors, or a complex rectifying action.

(2) To facilitate the analysis of the boundedness and convergence, we develop a novel analytical method based on CM and CEF. Compared with various conventional analytical methods merely based on CEF, the proposed method does not require the non-increasing property of CEF and can be used to obtain $\mathscr{L}_{\infty e}$-norm boundedness of the estimates and the inputs, which is more practical than $\mathscr{L}_{2e}$-norm boundedness in most existing works, e.g., Jin (2017, 2019) and Xing and Liu (2019).

(3) From a practical perspective, the smooth inputs are provided by our proposed adaptive ILC for the repetitive attitude tracking of the rigid spacecraft with a Sun-synchronous orbit. Compared with existing smoothed adaptive ILC in e.g., Jin (2017), the proposed method guarantees the iteration-independent smoothness, which implies that the approximation of $\mathrm{sgn}(\cdot)$ does not need to approach $\mathrm{sgn}(\cdot)$ when the iteration tends to infinity.

The remaining sections are organized as follows. In Section 2, some concepts of attitude control and the motion dynamics of spacecraft are introduced. In Section 3, the problem statement is presented, followed by the adaptive ILC design and convergence analysis in Section 4. Simulations and conclusions are given in Sections 5 and 6, respectively.

Notations. Let $\mathbb{Z}_+ = \{0, 1, 2, \ldots\}$ be the set of nonnegative integers, and $\boldsymbol{I}_3 \in \mathbb{R}^{3\times 3}$ be the identity matrix. For any $\boldsymbol{A} = \left[a_{ij}\right] \in \mathbb{R}^{m\times n}$, $\|\boldsymbol{A}\|$ denotes the spectral norm of $\boldsymbol{A}$. For any positive definite matrix $\boldsymbol{B} = \left[b_{ij}\right] \in \mathbb{R}^{m\times m}$, $\lambda_{\min}(\boldsymbol{B})$ denotes the minimal eigenvalue. $\mathbb{S}^3 = \{\boldsymbol{x} \in \mathbb{R}^4 : \|\boldsymbol{x}\| = 1\}$ denotes the three-sphere space. $SO(n)$ denotes the special orthogonal group. For any $\boldsymbol{x} = [x_i] \in \mathbb{R}^3$, the sign operator is defined as $\mathrm{sgn}(\boldsymbol{x}) = [\mathrm{sgn}(x_i)] \in \mathbb{R}^3$, the hyperbolic tangent operator is defined as $\tanh\left(\frac{\boldsymbol{x}}{\sigma}\right) = \left[\tanh\left(\frac{x_i}{\sigma}\right)\right] \in \mathbb{R}^3$ with $\sigma > 0$. $(\cdot)^\times$ is the vector cross-product operator such that $\boldsymbol{x}^\times \boldsymbol{y} = \boldsymbol{x}\times\boldsymbol{y}$ for any $\boldsymbol{x}, \boldsymbol{y} \in \mathbb{R}^3$.

2. Attitude dynamics and kinematics

In practical scenarios, quaternions $(\varepsilon, \boldsymbol{q}) \in \mathbb{R}\times\mathbb{R}^3$, lying in the non-Euclidean three-sphere space $\mathbb{S}^3$, are generally leveraged to describe orientations based on Euler's rotation theorem. As shown in Hughes (2004), any two Cartesian coordinate frames can be related by only one rotation about some fixed axis. In the present work, the orientation of the body-fixed frame $\mathcal{F}_B$ $(O - X_BY_BZ_B)$ with respect to the Earth-centered inertial frame $\mathcal{F}_I$ $(O - X_IY_IZ_I)$ can be represented by quaternions. Specifically, according to Hughes (2004), a quaternion can be represented as

$$\varepsilon = \cos\left(\frac{\varphi}{2}\right) \text{ and } \boldsymbol{q} = \boldsymbol{e}\sin\left(\frac{\varphi}{2}\right), \tag{1}$$

where $\boldsymbol{e} \in \mathbb{R}^3$ is the unit Euler axis (i.e., $\boldsymbol{e}^{\mathrm{T}}\boldsymbol{e} = 1$) and $\varphi \in \mathbb{R}$ is the Euler angle. From (1), $\varepsilon^2 + \boldsymbol{q}^{\mathrm{T}}\boldsymbol{q} = 1$ holds.

According to the above concepts, the attitude dynamics and kinematics of spacecraft can be presented as

$$\begin{aligned}
\boldsymbol{J}_k\dot{\boldsymbol{\omega}}_k(t) &= -\boldsymbol{\omega}_k^\times(t)\boldsymbol{J}_k\boldsymbol{\omega}_k(t) + \boldsymbol{u}_k(t) + \boldsymbol{d}_k(t)\\
\dot{\boldsymbol{q}}_k(t) &= \frac{1}{2}\left(\boldsymbol{q}_k^\times(t) + \varepsilon_k(t)\boldsymbol{I}_3\right)\boldsymbol{\omega}_k(t)\\
\dot{\varepsilon}_k(t) &= -\frac{1}{2}\boldsymbol{q}_k^{\mathrm{T}}(t)\boldsymbol{\omega}_k(t),
\end{aligned} \tag{2}$$

where $k \in \mathbb{Z}_+$ is the iteration index; $t \in [0, T]$ is the operation time with the terminal time T; $\varepsilon_k(t)$ and $\boldsymbol{q}_k(t)$ are the scalar part and the vector part of the quaternion, respectively; $\boldsymbol{\omega}_k(t) \in \mathbb{R}^3$ is the angular velocity of the spacecraft with respect to $\mathcal{F}_I$ as expressed in $\mathcal{F}_B$; $\boldsymbol{J}_k \in \mathbb{R}^{3\times 3}$ is the positive definite inertia matrix; $\boldsymbol{u}_k(t) \in \mathbb{R}^3$ denotes the control torque; and $\boldsymbol{d}_k(t) \in \mathbb{R}^3$ is the external disturbance.

3. Problem statement

3.1. Error kinematics and dynamics

Let $(\varepsilon_d(t), \boldsymbol{q}_d(t)) \in \mathbb{R}\times\mathbb{R}^3$ and $\boldsymbol{\omega}_d(t) \in \mathbb{R}^3$ denote the reference attitude quaternion and the reference angular velocity of the reference frame $\mathcal{F}_R$ $(O - X_RY_RZ_R)$ with respect to $\mathcal{F}_I$. Of note that

$(\varepsilon_d(t), \boldsymbol{q}_d(t))$ and $\boldsymbol{\omega}_d(t)$ satisfy the same kinematics as that in (2), and $\dot{\boldsymbol{\omega}}_d(t)$ exists. Generally, $\boldsymbol{\omega}_d(t)$ and $\dot{\boldsymbol{\omega}}_d(t)$ are supposed to be bounded for all $t \in [0, T]$. Moreover, let $(\delta\varepsilon_k(t), \delta\boldsymbol{q}_k(t)) \in \mathbb{R} \times \mathbb{R}^3$ and $\delta\boldsymbol{\omega}_k(t)$ be the quaternion error and the angular velocity error, respectively. With the quaternion multiplication rule in Hughes (2004), we obtain

$$\begin{aligned}
\delta\boldsymbol{q}_k(t) &= \varepsilon_d(t)\boldsymbol{q}_k(t) - \varepsilon_k(t)\boldsymbol{q}_d(t) + \boldsymbol{q}_k^{\times}(t)\boldsymbol{q}_d(t)\\
\delta\varepsilon_k(t) &= \varepsilon_d(t)\varepsilon_k(t) + \boldsymbol{q}_k^{\mathrm{T}}(t)\boldsymbol{q}_d(t)\\
\delta\boldsymbol{\omega}_k(t) &= \boldsymbol{\omega}_k(t) - \boldsymbol{R}_k(t)\boldsymbol{\omega}_d(t),
\end{aligned} \tag{3}$$

where $\boldsymbol{R}_k(t) \in SO(3)$ denotes the rotation matrix from $\mathcal{F}_R$ to $\mathcal{F}_B$ and is given by

$$\begin{aligned}
\boldsymbol{R}_k(t) = &\left(\delta\varepsilon_k(t)\delta\varepsilon_k(t) - \delta\boldsymbol{q}_k^{\mathrm{T}}(t)\delta\boldsymbol{q}_k(t)\right)\boldsymbol{I}_3\\
&+ 2\delta\boldsymbol{q}_k(t)\delta\boldsymbol{q}_k^{\mathrm{T}}(t) - 2\delta\varepsilon_k(t)\delta\boldsymbol{q}_k^{\times}(t).
\end{aligned} \tag{4}$$

Additionally, according to Hughes (2004), $\dot{\boldsymbol{R}}_k(t)$ is given by

$$\dot{\boldsymbol{R}}_k(t) = -\delta\boldsymbol{\omega}_k^{\times}(t)\boldsymbol{R}_k(t). \tag{5}$$

According to (2)–(5), the attitude tracking error system of spacecraft in terms of $\delta\varepsilon_k(t)$ and $\delta\boldsymbol{q}_k(t)$ can be obtained as

$$\begin{aligned}
\boldsymbol{J}_k\delta\dot{\boldsymbol{\omega}}_k(t) = &\boldsymbol{J}_k\left(\delta\boldsymbol{\omega}_k^{\times}(t)\boldsymbol{R}_k(t)\boldsymbol{\omega}_d(t) - \boldsymbol{R}_k(t)\dot{\boldsymbol{\omega}}_d(t)\right)\\
&- \boldsymbol{\omega}_k^{\times}(t)\boldsymbol{J}_k\boldsymbol{\omega}_k(t) + \boldsymbol{u}_k(t) + \boldsymbol{d}_k(t)\\
\delta\dot{\boldsymbol{q}}_k(t) = &\frac{1}{2}\left(\delta\boldsymbol{q}_k^{\times}(t) + \delta\varepsilon_k(t)\boldsymbol{I}_3\right)\delta\boldsymbol{\omega}_k(t)\\
\delta\dot{\varepsilon}_k(t) = &-\frac{1}{2}\delta\boldsymbol{q}_k^{\mathrm{T}}(t)\delta\boldsymbol{\omega}_k(t).
\end{aligned} \tag{6}$$

From (3), (4), and the symmetry of $\boldsymbol{J}_k$, we obtain the following lemma including three useful properties (See Zhang et al., 2022 for the detailed proof).

Lemma 1. *For the attitude error kinematics and dynamics (6), the following statements hold:*

- $\delta\boldsymbol{q}_k^{\mathrm{T}}(t)\delta\boldsymbol{q}_k(t) + \delta\varepsilon_k(t)\delta\varepsilon_k(t) = 1$.
- *The rotation matrix $\boldsymbol{R}_k(t)$ is orthogonal.*
- $(\boldsymbol{R}_k(t)\boldsymbol{\omega}_d(t))^{\times}\boldsymbol{J}_k + \boldsymbol{J}_k(\boldsymbol{R}_k(t)\boldsymbol{\omega}_d(t))^{\times}$ *is skew symmetric.*

Another useful lemma about the hyperbolic tangent operator in Li et al. (2016) is recalled as follows.

Lemma 2. *For any $\boldsymbol{x} \in \mathbb{R}^n$ with $n \in \mathbb{Z}_+\backslash\{0\}$, the following inequality holds for any $\sigma > 0$:*

$$0 \leqslant \boldsymbol{x}^{\mathrm{T}}\operatorname{sgn}(\boldsymbol{x}) - \boldsymbol{x}^{\mathrm{T}}\tanh\left(\frac{\boldsymbol{x}}{\sigma}\right) \leqslant n\epsilon\sigma,$$

where $\epsilon = e^{-(\epsilon+1)}$, i.e., $\epsilon \approx 0.2785$.

3.2. Problem statement

The objective of this paper is to design a chattering-free adaptive ILC method for the attitude tracking error system (6), with which the tracking errors can be uniformly bounded and converge to a neighborhood of the origin along the iteration axis in the presence of initial state errors, i.e.,

$$\begin{cases}
\sup_{k\in\mathbb{Z}_+, t\in[0,T]} \left\|\delta\boldsymbol{q}_k(t)\right\| \leqslant \beta_{\delta q}\\
\sup_{k\in\mathbb{Z}_+, t\in[0,T]} \|\delta\boldsymbol{\omega}_k(t)\| \leqslant \beta_{\delta\omega}
\end{cases} \tag{7}$$

and

$$\begin{cases}
\limsup_{k\to\infty} \left\|\delta\boldsymbol{q}_k(t)\right\| \leqslant \beta_{\delta q_{\sup}}\\
\limsup_{k\to\infty} \|\delta\boldsymbol{\omega}_k(t)\| \leqslant \beta_{\delta\omega_{\sup}}
\end{cases} \quad \forall t \in [0, T] \tag{8}$$

for some finite $\beta_{\delta q} > 0$, $\beta_{\delta\omega} > 0$, $\beta_{\delta q_{\sup}} > 0$ and $\beta_{\delta\omega_{\sup}} > 0$.

To facilitate the design of the attitude control law, we introduce the following assumptions.

Assumption 3. Let initial state errors be uniformly bounded along the iteration axis, namely, there exist two finite (unknown) constants $\beta_{\delta q0} > 0$ and $\beta_{\delta\omega0} > 0$ such that

$$\sup_{k\in\mathbb{Z}_+}\left\|\delta\boldsymbol{q}_k(0)\right\| \leqslant \beta_{\delta q0} \quad \text{and} \quad \sup_{k\in\mathbb{Z}_+}\|\delta\boldsymbol{\omega}_k(0)\| \leqslant \beta_{\delta\omega0}.$$

Assumption 4. The external disturbance $\boldsymbol{d}_k(t)$ and the inertia matrix $\boldsymbol{J}_k$ are uniformly bounded along the iteration axis, i.e.,

$$\sup_{k\in\mathbb{Z}_+}\|\boldsymbol{d}_k(t)\| \leqslant \beta_d(t) \quad \text{and} \quad \sup_{k\in\mathbb{Z}_+}\left\|\boldsymbol{J}_k\right\| \leqslant \beta_J \tag{9}$$

hold for some finite (unknown) bounds $\beta_d(t) > 0$ and $\beta_J > 0$ over $t \in [0, T]$.

Remark 5. For conventional adaptive ILC, the identical initial condition (i.e., $\beta_{\delta q0} = 0$ and $\beta_{\delta\omega0} = 0$) is generally assumed to ensure the perfect tracking control performance, which does not always hold in most of the practical applications (Jin, 2017; Yang et al., 2015). By comparison, Assumption 3 is more general than the identical initial condition. In addition, the uniform bounds, i.e., $\beta_{\delta q0}$ and $\beta_{\delta\omega0}$, are not required to design the controller, which is different from Xie and Sun (2009) and Zhang et al. (2022).

Remark 6. Assumption 4 is mild in the area of spacecraft (Hu et al., 2013; Petersen et al., 2017; Zhao & Duan, 2021). In contrast to the existing works with assumptions of constant and known inertia matrix, e.g., Abdessameud, Tayebi, and Polushin (2012), the present work considers an iteration-varying inertia matrix with some finite but unknown bound, which is more practical for attitude tracking.

4. Controller design and convergence

In this section, an adaptive controller and a parametric learning law are developed for the repetitive attitude tracking task. Further, a novel analytical method consisting of CEF and CM is exploited to demonstrate the robust tracking performance in the presence of initial state errors and to effectively avoid the chattering phenomenon.

To achieve the aforementioned objectives (7) and (8), we develop a novel adaptive controller as

$$\boldsymbol{u}_k(t) = -k_p\delta\varepsilon_k(t)\delta\boldsymbol{q}_k(t) - k_d\delta\boldsymbol{\omega}_k(t) - \hat{\theta}_k(t)\tanh\left(\frac{\delta\boldsymbol{\omega}_k(t)}{\sigma}\right), \tag{10}$$

where $k_p \in \mathbb{R}$ and $k_d \in \mathbb{R}$ are two positive controller parameters, $\sigma \in \mathbb{R}$ is an arbitrarily small positive scalar, and $\hat{\theta}_k(t) \in \mathbb{R}$ is the estimate of the system uncertainty $\theta(t) \in \mathbb{R}$ satisfying

$$\theta(t) \geqslant \beta_J\left(\|\boldsymbol{\omega}_d(t)\|^2 + \|\dot{\boldsymbol{\omega}}_d(t)\|\right) + \beta_d(t) \tag{11}$$

with $\beta_d(t)$ and β_J defined in (9).

The learning law for $\hat{\theta}_k(t)$ along the iteration axis is designed as, for all $k \in \mathbb{Z}_+\backslash\{0\}$,

$$\begin{aligned}
\hat{\theta}_k(t) &= (1-\gamma_2)\,\hat{\theta}_{k-1}(t) + \gamma_1\delta\boldsymbol{\omega}_k^{\mathrm{T}}(t)\tanh\left(\frac{\delta\boldsymbol{\omega}_k(t)}{\sigma}\right)\\
\hat{\theta}_0(t) &= 0, \quad \forall t \in [0, T],
\end{aligned} \tag{12}$$

where $\gamma_1 > 0$ and $0 < \gamma_2 < 1$ are the learning gain and the reduction factor, respectively. It is worth noticing that, based on (12), $\hat{\theta}_k(t) \geqslant 0$ holds for all $k \in \mathbb{Z}_+$ and all $t \in [0, T]$ according to the definitions of γ_1 and γ_2.

Remark 7. It is worth noticing that the proposed adaptive ILC method consisting of (10) and (12) does not involve the inertia matrix and the uniform bounds of initial state errors. From this point of view, the proposed method is more robust and practical

than these involving the boundary layer in Xie and Sun (2009) or the deadzone mechanism in Zhang et al. (2022), especially when actual initial state errors are larger than nominal uniform bounds.

Remark 8. Note that $\tanh(\cdot)$ is generally employed to deal with the saturation (He, Meng, He, & Ge, 2018) and the non-smoothness problem (Li et al., 2016) along the time axis. Unfortunately, when $\tanh(\cdot)$ is employed in the conventional adaptive ILC in Jin (2017), Xing and Liu (2019), the boundedness and the monotonicity of CEF cannot be guaranteed. To address this problem, we establish a novel analytical method consisting of CEF and CM, where the reduction factor is used to construct CM and ensure the monotonicity.

With the proposed chattering-free adaptive ILC method, the following result can be achieved, which shows the robust tracking performance in the presence of initial state errors, system uncertainties, and external disturbances.

Theorem 9. *Consider the attitude tracking error system (6) under Assumptions 3 and 4, let the proposed controller (10) together with the parametric learning law (12) be applied. Then the robust tracking objectives presented in (7) and (8) can be achieved.*

To show the evolution of the attitude tracking errors, we develop the following CEF

$$W_k(t) = V_k(t) + \frac{1}{2\gamma_1}\int_0^t \tilde{\theta}_k^2(\tau)\mathrm{d}\tau \tag{13}$$

with

$$\tilde{\theta}_k(t) \triangleq \theta(t) - \hat{\theta}_k(t) \tag{14}$$

representing the estimation error and $V_k(t)$ defined as

$$V_k(t) = V_{q,k}(t) + V_{\omega,k}(t) \tag{15}$$

where

$$\begin{aligned} V_{q,k}(t) &\triangleq k_p \delta\boldsymbol{q}_k^{\mathrm{T}}(t)\delta\boldsymbol{q}_k(t) \\ V_{\omega,k}(t) &\triangleq \frac{1}{2}\delta\boldsymbol{\omega}_k^{\mathrm{T}}(t)\boldsymbol{J}_k\delta\boldsymbol{\omega}_k(t). \end{aligned} \tag{16}$$

Proof of Theorem 9. The analysis process using the hybrid analytical method of CEF and CM is divided into three parts. The first part shows the evolution along the iteration axis, which is followed by the analysis of boundedness for the CEF at the initial iteration. In the third part, the convergence of the tracking errors is presented.

Part (1): Evolution of $W_k(t)$ along the iteration axis.

According to the definition of $W_k(t)$ presented in (13), we can obtain that the difference between $W_k(t)$ and $W_{k-1}(t)$ can be calculated as

$$\Delta W_k(t) \triangleq W_k(t) - W_{k-1}(t),$$

which leads to

$$\begin{aligned} \Delta W_k(t) = &\int_0^t \dot{V}_k(\tau)\mathrm{d}\tau + V_k(0) - V_{k-1}(t) \\ &- \frac{1}{2\gamma_1}\int_0^t \left(2\bar{\theta}_k(\tau)\tilde{\theta}_k(\tau) + \bar{\theta}_k^2(\tau)\right)\mathrm{d}\tau, \end{aligned} \tag{17}$$

where $\bar{\theta}_k(t) \triangleq \hat{\theta}_k(t) - \hat{\theta}_{k-1}(t)$. According to (12), we have

$$\bar{\theta}_k(t) = \gamma_1 \delta\boldsymbol{\omega}_k^{\mathrm{T}}(t)\tanh\left(\frac{\delta\boldsymbol{\omega}_k(t)}{\sigma}\right) - \gamma_2\hat{\theta}_{k-1}(t). \tag{18}$$

For the further analysis of (17), let us first look into $\dot{V}_{q,k}(t)$. By Lemma 1, (6), and (16), it is not difficult to derive

$$\dot{V}_{q,k}(t) = k_p \delta\varepsilon_k(t)\delta\boldsymbol{q}_k^{\mathrm{T}}(t)\delta\boldsymbol{\omega}_k(t). \tag{19}$$

Similarly, we can obtain

$$\begin{aligned} \dot{V}_{\omega,k}(t) = &\delta\boldsymbol{\omega}_k^{\mathrm{T}}(t)\boldsymbol{J}_k\left(\delta\boldsymbol{\omega}_k^{\times}(t)\boldsymbol{R}_k(t)\boldsymbol{\omega}_d(t) - \boldsymbol{R}_k(t)\dot{\boldsymbol{\omega}}_d(t)\right) \\ &- \delta\boldsymbol{\omega}_k^{\mathrm{T}}(t)\boldsymbol{\omega}_k^{\times}(t)\boldsymbol{J}_k\boldsymbol{\omega}_k(t) + \delta\boldsymbol{\omega}_k^{\mathrm{T}}(t)\boldsymbol{d}_k(t) + \delta\boldsymbol{\omega}_k^{\mathrm{T}}(t)\boldsymbol{u}_k(t). \end{aligned} \tag{20}$$

Moreover, according to the property of the vector cross-product operator, one can reasonably obtain

$$\begin{aligned} &\delta\boldsymbol{\omega}_k^{\mathrm{T}}(t)\boldsymbol{J}_k\left(\delta\boldsymbol{\omega}_k^{\times}(t)\boldsymbol{R}_k(t)\boldsymbol{\omega}_d(t) - \boldsymbol{R}_k(t)\dot{\boldsymbol{\omega}}_d(t)\right) \\ &= -\delta\boldsymbol{\omega}_k^{\mathrm{T}}(t)\boldsymbol{J}_k\left(\boldsymbol{R}_k(t)\boldsymbol{\omega}_d(t)\right)^{\times}\delta\boldsymbol{\omega}_k(t) - \delta\boldsymbol{\omega}_k^{\mathrm{T}}(t)\boldsymbol{J}_k\boldsymbol{R}_k(t)\dot{\boldsymbol{\omega}}_d(t) \end{aligned} \tag{21}$$

and

$$\begin{aligned} &\delta\boldsymbol{\omega}_k^{\mathrm{T}}(t)\boldsymbol{\omega}_k^{\times}(t)\boldsymbol{J}_k\boldsymbol{\omega}_k(t) \\ &= \delta\boldsymbol{\omega}_k^{\mathrm{T}}(t)\left(\boldsymbol{R}_k(t)\boldsymbol{\omega}_d(t)\right)^{\times}\boldsymbol{J}_k\delta\boldsymbol{\omega}_k(t) \\ &\quad + \delta\boldsymbol{\omega}_k^{\mathrm{T}}(t)\left(\boldsymbol{R}_k(t)\boldsymbol{\omega}_d(t)\right)^{\times}\boldsymbol{J}_k\boldsymbol{R}_k(t)\boldsymbol{\omega}_d(t), \end{aligned} \tag{22}$$

where (3) is applied. To proceed, we have

$$\begin{aligned} \dot{V}_{\omega,k}(t) = &-\delta\boldsymbol{\omega}_k^{\mathrm{T}}(t)\boldsymbol{J}_k\left(\boldsymbol{R}_k(t)\boldsymbol{\omega}_d(t)\right)^{\times}\delta\boldsymbol{\omega}_k(t) \\ &-\delta\boldsymbol{\omega}_k^{\mathrm{T}}(t)\left(\boldsymbol{R}_k(t)\boldsymbol{\omega}_d(t)\right)^{\times}\boldsymbol{J}_k\delta\boldsymbol{\omega}_k(t) \\ &-\delta\boldsymbol{\omega}_k^{\mathrm{T}}(t)\left(\boldsymbol{R}_k(t)\boldsymbol{\omega}_d(t)\right)^{\times}\boldsymbol{J}_k\boldsymbol{R}_k(t)\boldsymbol{\omega}_d(t) \\ &-\delta\boldsymbol{\omega}_k^{\mathrm{T}}(t)\boldsymbol{J}_k\boldsymbol{R}_k(t)\dot{\boldsymbol{\omega}}_d(t) + \delta\boldsymbol{\omega}_k^{\mathrm{T}}(t)\boldsymbol{d}_k(t) + \delta\boldsymbol{\omega}_k^{\mathrm{T}}(t)\boldsymbol{u}_k(t) \end{aligned} \tag{23}$$

by combining (21) and (22) into (20). According to Lemma 1, (23) leads to

$$\begin{aligned} \dot{V}_{\omega,k}(t) \leqslant &\left(\|\boldsymbol{J}_k\|\,\|\boldsymbol{\omega}_d(t)\|^2 + \|\boldsymbol{J}_k\|\,\|\dot{\boldsymbol{\omega}}_d(t)\| + \|\boldsymbol{d}_k(t)\|\right)\|\delta\boldsymbol{\omega}_k^{\mathrm{T}}(t)\| \\ &+ \delta\boldsymbol{\omega}_k^{\mathrm{T}}(t)\boldsymbol{u}_k(t). \end{aligned} \tag{24}$$

Taking the sum of (19) and (24), we have

$$\begin{aligned} \dot{V}_k(t) \leqslant &\left(\|\boldsymbol{J}_k\|\,\|\boldsymbol{\omega}_d(t)\|^2 + \|\boldsymbol{J}_k\|\,\|\dot{\boldsymbol{\omega}}_d(t)\| + \|\boldsymbol{d}_k(t)\|\right)\|\delta\boldsymbol{\omega}_k^{\mathrm{T}}(t)\| \\ &+ k_p\delta\varepsilon_k(t)\delta\boldsymbol{\omega}_k^{\mathrm{T}}(t)\delta\boldsymbol{q}_k(t) + \delta\boldsymbol{\omega}_k^{\mathrm{T}}(t)\boldsymbol{u}_k(t), \end{aligned}$$

with substituting (11) into which we have

$$\dot{V}_k(t) \leqslant \theta(t)\|\delta\boldsymbol{\omega}_k^{\mathrm{T}}(t)\| + k_p\delta\varepsilon_k(t)\delta\boldsymbol{\omega}_k^{\mathrm{T}}(t)\delta\boldsymbol{q}_k(t) + \delta\boldsymbol{\omega}_k^{\mathrm{T}}(t)\boldsymbol{u}_k(t). \tag{25}$$

To proceed, (25) and the control input (10) yield

$$\begin{aligned} \dot{V}_k(t) \leqslant &\theta(t)\|\delta\boldsymbol{\omega}_k^{\mathrm{T}}(t)\| - \hat{\theta}_k(t)\delta\boldsymbol{\omega}_k^{\mathrm{T}}(t)\tanh\left(\frac{\delta\boldsymbol{\omega}_k(t)}{\sigma}\right) \\ &- k_d\delta\boldsymbol{\omega}_k^{\mathrm{T}}(t)\delta\boldsymbol{\omega}_k(t), \end{aligned} \tag{26}$$

which, together with (17) and (18), leads to

$$\begin{aligned} \Delta W_k(t) \leqslant &-\int_0^t \tilde{\theta}_k(\tau)\delta\boldsymbol{\omega}_k^{\mathrm{T}}(\tau)\tanh\left(\frac{\delta\boldsymbol{\omega}_k(\tau)}{\sigma}\right)\mathrm{d}\tau \\ &+ \frac{\gamma_2}{\gamma_1}\int_0^t \tilde{\theta}_k(\tau)\hat{\theta}_{k-1}(\tau)\mathrm{d}\tau - \frac{1}{2\gamma_1}\int_0^t \bar{\theta}_k^2(\tau)\mathrm{d}\tau \\ &+ \int_0^t \theta(\tau)\delta\boldsymbol{\omega}_k^{\mathrm{T}}(\tau)\,\mathrm{sgn}\left(\delta\boldsymbol{\omega}_k(\tau)\right)\mathrm{d}\tau + V_k(0) \\ &- \int_0^t \hat{\theta}_k(\tau)\delta\boldsymbol{\omega}_k^{\mathrm{T}}(\tau)\tanh\left(\frac{\delta\boldsymbol{\omega}_k(\tau)}{\sigma}\right)\mathrm{d}\tau \\ &- \int_0^t k_d\delta\boldsymbol{\omega}_k^{\mathrm{T}}(\tau)\delta\boldsymbol{\omega}_k(\tau)\mathrm{d}\tau - V_{k-1}(t). \end{aligned} \tag{27}$$

According to Lemma 2, we have

$$\delta\boldsymbol{\omega}_k^{\mathrm{T}}(t)\left(\mathrm{sgn}\left(\delta\boldsymbol{\omega}_k(t)\right) - \tanh\left(\frac{\delta\boldsymbol{\omega}_k(t)}{\sigma}\right)\right) \leqslant 3\epsilon\sigma. \tag{28}$$

Inserting (14) and (28) into (27), we can verify

$$\begin{aligned} \Delta W_k(t) \leqslant &\frac{\gamma_2}{\gamma_1}\int_0^t \tilde{\theta}_k(\tau)\hat{\theta}_{k-1}(\tau)\mathrm{d}\tau - \frac{1}{2\gamma_1}\int_0^t \bar{\theta}_k^2(\tau)\mathrm{d}\tau \\ &- \int_0^t k_d\delta\boldsymbol{\omega}_k^{\mathrm{T}}(\tau)\delta\boldsymbol{\omega}_k(\tau)\mathrm{d}\tau - V_{k-1}(t) + \beta_1(t), \end{aligned} \tag{29}$$

where $\beta_1(t)$ defined as

$$\beta_1(t) \triangleq \int_0^t 3\epsilon\sigma\theta(\tau)\mathrm{d}\tau + k_p\beta_{\delta q0}^2 + \frac{1}{2}\beta_J\beta_{\delta\omega 0}^2 \tag{30}$$

is bounded according to (15), (16), and Assumptions 3 and 4. $\Delta W_k(t)$ in (29) does not meet the non-increasing condition when $\beta_1(t) \neq 0$. This makes the conventional CEF analysis approach fail to work.

Considering (14) and (18) again, we have

$$\tilde{\theta}_k(t) = \tilde{\theta}_{k-1}(t) - \gamma_1\delta\boldsymbol{\omega}_k^{\mathrm{T}}(t)\tanh\left(\frac{\delta\boldsymbol{\omega}_k(t)}{\sigma}\right) + \gamma_2\hat{\theta}_{k-1}(t),$$

which, together with (29), leads to

$$\begin{aligned}\Delta W_k(t) \leqslant\ & \frac{\gamma_2}{\gamma_1}\int_0^t \tilde{\theta}_{k-1}(\tau)\hat{\theta}_{k-1}(\tau)\mathrm{d}\tau + \frac{\gamma_2^2}{\gamma_1}\int_0^t \hat{\theta}_{k-1}^2(\tau)\mathrm{d}\tau \\ & - \gamma_2\int_0^t \delta\boldsymbol{\omega}_k^{\mathrm{T}}(\tau)\tanh\left(\frac{\delta\boldsymbol{\omega}_k(\tau)}{\sigma}\right)\hat{\theta}_{k-1}(\tau)\mathrm{d}\tau \\ & - \frac{1}{2\gamma_1}\int_0^t \bar{\theta}_k^2(\tau)\mathrm{d}\tau - V_{k-1}(t) + \beta_1(t) \\ & - \int_0^t k_d\delta\boldsymbol{\omega}_k^{\mathrm{T}}(\tau)\delta\boldsymbol{\omega}_k(\tau)\mathrm{d}\tau,\end{aligned} \tag{31}$$

Moreover, according to (18), we have

$$\begin{aligned}-\frac{1}{2\gamma_1}\int_0^t \bar{\theta}_k^2(\tau)\mathrm{d}\tau \leqslant\ & \gamma_2\int_0^t \delta\boldsymbol{\omega}_k^{\mathrm{T}}(\tau)\tanh\left(\frac{\delta\boldsymbol{\omega}_k(\tau)}{\sigma}\right)\hat{\theta}_{k-1}(\tau)\mathrm{d}\tau \\ & - \frac{\gamma_2^2}{2\gamma_1}\int_0^t \hat{\theta}_{k-1}^2(\tau)\mathrm{d}\tau,\end{aligned}$$

with substituting which into (31), we can obtain

$$\begin{aligned}\Delta W_k(t) \leqslant\ & \frac{\gamma_2}{\gamma_1}\int_0^t \tilde{\theta}_{k-1}(\tau)\hat{\theta}_{k-1}(\tau)\mathrm{d}\tau + \frac{\gamma_2^2}{2\gamma_1}\int_0^t \hat{\theta}_{k-1}^2(\tau)\mathrm{d}\tau \\ & - V_{k-1}(t) + \beta_1(t) - \int_0^t k_d\delta\boldsymbol{\omega}_k^{\mathrm{T}}(\tau)\delta\boldsymbol{\omega}_k(\tau)\mathrm{d}\tau.\end{aligned}$$

Further, according to the definitions of γ_1 and γ_2, we have

$$\begin{aligned}\Delta W_k(t) \leqslant\ & \beta_1(t) + \beta_2(t) - V_{k-1}(t) - \frac{\gamma_2}{2\gamma_1}\int_0^t \tilde{\theta}_{k-1}^2(\tau)\mathrm{d}\tau \\ & - \int_0^t k_d\delta\boldsymbol{\omega}_k^{\mathrm{T}}(\tau)\delta\boldsymbol{\omega}_k(\tau)\mathrm{d}\tau,\end{aligned} \tag{32}$$

where

$$\beta_2(t) \triangleq \frac{\gamma_2}{2\gamma_1}\int_0^t \theta^2(\tau)\mathrm{d}\tau. \tag{33}$$

To proceed, (13) and (32) lead to

$$\begin{aligned}W_k(t) \leqslant\ & (1-\gamma_2)\,W_{k-1}(t) - (1-\gamma_2)\,V_{k-1}(t) \\ & - \int_0^t k_d\delta\boldsymbol{\omega}_k^{\mathrm{T}}(\tau)\delta\boldsymbol{\omega}_k(\tau)\mathrm{d}\tau + \beta_1(t) + \beta_2(t).\end{aligned} \tag{34}$$

As a result, one can obtain

$$\begin{aligned}W_k(t) \leqslant\ & (1-\gamma_2)^{k-1}\,W_1(t) + \frac{1-(1-\gamma_2)^{k-1}}{\gamma_2} \\ & \times(\beta_1(t)+\beta_2(t)).\end{aligned} \tag{35}$$

In addition, from the definition of γ_2, we have

$$W_k(t) \leqslant W_1(t) + \frac{\beta_1(t)+\beta_2(t)}{\gamma_2}. \tag{36}$$

To prove the boundedness of $W_k(t)$, we should ensure the boundedness of $W_1(t)$, which can be analyzed in Part (2).

Part (2): Boundedness of $\delta\boldsymbol{q}_k(t)$, $\delta\boldsymbol{\omega}_k(t)$, and $\boldsymbol{u}_k(t)$.

According to (12), the system runs from $k = 0$ whereas the learning begins from $k = 1$, therefore we should consider the boundedness of $W_1(t)$ and $W_0(t)$. The analyses are similar, thus we just take $W_1(t)$ as an example.

According to (13), the derivative of $W_1(t)$ is calculated as

$$\dot{W}_1(t) = \dot{V}_1(t) + \frac{1}{2\gamma_1}\tilde{\theta}_1^2(t). \tag{37}$$

According to (26), (37) can be rewritten as

$$\begin{aligned}\dot{W}_1(t) \leqslant\ & \theta(t)\delta\boldsymbol{\omega}_1^{\mathrm{T}}(t)\,\mathrm{sgn}\,(\delta\boldsymbol{\omega}_1(t)) + \frac{1}{2\gamma_1}\tilde{\theta}_1^2(t) \\ & - \hat{\theta}_1(t)\delta\boldsymbol{\omega}_1^{\mathrm{T}}(t)\tanh\left(\frac{\delta\boldsymbol{\omega}_1(t)}{\sigma}\right) - k_d\delta\boldsymbol{\omega}_1^{\mathrm{T}}(t)\delta\boldsymbol{\omega}_1(t).\end{aligned} \tag{38}$$

By applying (28) again, we can further rewrite (38) as

$$\dot{W}_1(t) \leqslant 3\epsilon\sigma\theta(t) + \tilde{\theta}_1(t)\delta\boldsymbol{\omega}_1^{\mathrm{T}}(t)\tanh\left(\frac{\delta\boldsymbol{\omega}_1(t)}{\sigma}\right) + \frac{1}{2\gamma_1}\tilde{\theta}_1^2(t). \tag{39}$$

According to (12), we have

$$\hat{\theta}_1(t) = \gamma_1\delta\boldsymbol{\omega}_1^{\mathrm{T}}(t)\tanh\left(\frac{\delta\boldsymbol{\omega}_1(t)}{\sigma}\right) \tag{40}$$

for all $t \in [0, T]$, which, together with (39), yields

$$\begin{aligned}\dot{W}_1(t) \leqslant\ & 3\epsilon\sigma\theta(t) + \left(\hat{\theta}_1(t) + \frac{1}{2}\tilde{\theta}_1(t)\right)\frac{1}{\gamma_1}\tilde{\theta}_1(t) \\ \leqslant\ & 3\epsilon\sigma\theta(t) + \frac{1}{2\gamma_1}\theta^2(t).\end{aligned} \tag{41}$$

where (14) and Young's inequality are applied.

Therefore, the boundedness of $\dot{W}_1(t)$ can be implied by the boundedness of $\theta(t)$, which thus leads to the uniform boundedness of $W_1(t)$ over $[0, T]$. In the similar way, the uniform boundedness of $W_0(t)$ over $[0, T]$ can also be obtained. These two facts, together with (36), show that $W_k(t)$ is uniformly bounded for $t \in [0, T]$ and $k \in \mathbb{Z}_+$. As a consequence, (7) can be derived naturally according to (13), (15), (16), and β_J defined in Assumption 4, which implies the uniform boundedness properties of the attitude tracking errors $\delta\boldsymbol{q}_k(t)$ and $\delta\boldsymbol{\omega}_k(t)$.

Furthermore, we obtain that $\gamma_1\delta\boldsymbol{\omega}_k^{\mathrm{T}}(t)\tanh\left(\frac{\delta\boldsymbol{\omega}_k(t)}{\sigma}\right) \leqslant \gamma_1\delta\boldsymbol{\omega}_k^{\mathrm{T}}(t)\,\mathrm{sgn}\,(\delta\boldsymbol{\omega}_k(t))$ is bounded for all $t \in [0, T]$ and all $k \in \mathbb{Z}_+$ because of the boundedness of $\delta\boldsymbol{\omega}_k(t)$. Revisiting (12), it is not hard to verify the boundedness of the estimation error $\hat{\theta}_k(t)$ for all $t \in [0, T]$ and all $k \in \mathbb{Z}_+$ according to $0 < \gamma_2 < 1$. Based on the boundedness property of $\delta\boldsymbol{q}_k(t)$, $\delta\boldsymbol{\omega}_k(t)$, and $\hat{\theta}_k(t)$, we can derive that the control input $\boldsymbol{u}_k(t)$ is bounded from (10).

Part (3): Convergence of $\delta\boldsymbol{\omega}_k(t)$ and $\delta\boldsymbol{q}_k(t)$.

From the definition of γ_2 and the boundedness of $W_1(t)$, we can obtain

$$\limsup_{k\to\infty} W_k(t) \leqslant \frac{\beta_1(t)+\beta_2(t)}{\gamma_2}, \quad \forall t \in [0, T] \tag{42}$$

according to (35). Therefore, we have

$$\begin{cases}\limsup_{k\to\infty}\left\|\delta\boldsymbol{q}_k(t)\right\| \leqslant \beta_{\delta q_{\sup}}(t) \\ \limsup_{k\to\infty}\left\|\delta\boldsymbol{\omega}_k(t)\right\| \leqslant \beta_{\delta\omega_{\sup}}(t)\end{cases} \quad \forall t \in [0, T] \tag{43}$$

where

$$\beta_{\delta q_{\sup}}(t) \leqslant \left(\frac{\beta_1(t)+\beta_2(t)}{\gamma_2 k_p}\right)^{\frac{1}{2}} \tag{44}$$

and

$$\beta_{\delta\omega_{\sup}}(t) \leqslant \left(2\frac{\beta_1(t)+\beta_2(t)}{\gamma_2\lambda_{\min}(\boldsymbol{J}_k)}\right)^{\frac{1}{2}}. \tag{45}$$

Additionally, of note that the results are robust and the obtained upper bounds seem conservative owing to the term $\frac{1}{2\gamma_1}\int_0^t \tilde{\theta}_k^2(\tau)\mathrm{d}\tau$ in (13). Despite this issue, according to the definitions of $\beta_1(t)$ in (30) and $\beta_2(t)$ in (33), if the initial state errors are small enough, and σ and γ_2 are selected to be arbitrarily close to zero, the attitude tracking performance is further improved according to the boundedness of $W_k(t)$ and $\Delta W_k(t) \leqslant \beta_1(t) + \beta_2(t) - V_{k-1}(t)$ derived from (32). The proof is complete.

Remark 10. It is worth noting that if the conventional adaptive ILC is used when $\beta_1(t) \neq 0$, that is, $\gamma_2 = 0$, then (29) collapses into the following inequality $\Delta W_k(t) \leqslant -V_{k-1}(t) + \beta_1(t)$. However, under this inequality condition, the boundedness of $W_k(t)$ cannot be obtained with CEF methods any longer. This issue can be handled thanks to $-\gamma_2\hat{\theta}_{k-1}(t)$ in this work.

Remark 11. The uniform boundedness ($\mathscr{L}_{\infty e}$-norm boundedness) of CEF is more practical than $\mathscr{L}_{2e}$-norm boundedness introduced in conventional adaptive ILC schemes, e.g., Jin (2019), Tayebi (2004), Xing and Liu (2019) and Yang et al. (2015). Compared with $\mathscr{L}_{2e}$-norm, the uniform boundedness is able to guarantee the $\mathscr{L}_{\infty e}$-norm of the inputs.

5. Verification through uncertain spacecraft

In this section, the effectiveness of the proposed adaptive ILC method can be verified through spacecraft operated in one Sun-synchronous orbit, in which the spacecraft repeatedly passes over any given area of the Earth's surface at the same local mean solar time. In order to perform some specific tasks repetitively, such as imaging (Wu et al., 2015) and power transmission (Li et al., 2021), the spacecraft is required to periodically track the predefined attitude trajectory over a fixed time duration such that the OZ_B points to the desired areas.

The aforementioned Sun-synchronous orbit can be given with a semimajor axis of 6778.20 km, an eccentricity of zero, an inclination of 97.64 deg, a right ascension of the ascending node of 50.00 deg, an argument of periapsis of zero, and a true anomaly of zero.

The predefined attitude trajectory is assumed to be generated by $\varepsilon_d(0) = 0.66$ and $\boldsymbol{q}_d(0) = [0.34 \ -0.62 \ 0.25]^{\mathrm{T}}$ and

$$\boldsymbol{\omega}_d(t) = \begin{bmatrix} \frac{\pi}{8}\cdot\frac{\pi}{400}\sin(\frac{\pi}{400}t) \\ -\omega'\cos(-\frac{\pi}{8}\cos(\frac{\pi}{400}t)+\frac{\pi}{8}) \\ \omega'\sin(-\frac{\pi}{8}\cos(\frac{\pi}{400}t)+\frac{\pi}{8}) \end{bmatrix} \text{ rad/s},$$

where the mean motion ω' is 0.0011. $(\varepsilon_d(t), \boldsymbol{q}_d(t))$ can be obtained based on the attitude kinematics. Additionally, the time duration is selected to be $[0, 800]$ s.

The unknown inertia matrix $\boldsymbol{J}_k$ of the spacecraft can be iteration-varying and uniformly bounded along the iteration axis and thus is supposed to be $\boldsymbol{J}_k = \boldsymbol{J} + \Delta\boldsymbol{J}_k$ where

$$\boldsymbol{J} = \begin{bmatrix} 20 & 2 & 1 \\ 2 & 15 & 3 \\ 1 & 3 & 15 \end{bmatrix} \text{ kg m}^2$$

is unknown and $\Delta\boldsymbol{J}_k \in \mathbb{R}^{3\times 3}$ is a symmetric matrix, each element of which can be arbitrary and bounded by 0.5 kg $\cdot$ m^2. Moreover, initial state errors are arbitrary but bounded by $\beta_{\delta q0} = 0.001$ and $\beta_{\delta\omega 0} = 0.001$ rad/s.

For the sake of simplicity, the external disturbance $\boldsymbol{d}_k(t)$ upon three axes are taken with the periods of 40, 50, 100 s and the magnitudes of 0.1, 0.05, 0.05 N m, and the initial phases of the disturbances can be arbitrary. This setting is consistent with Assumption 4.

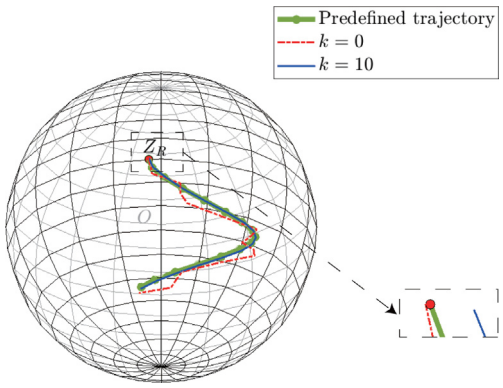

Fig. 1. Pointing trajectories on attitude sphere from almost identical initial attitude. Red dot: the starting point of the reference trajectory. (For interpretation of the references to color in this figure legend, the reader is referred to the web version of this article.)

According to (12), $\hat{\theta}_k(t) > \hat{\theta}_{k-1}(t)$ holds when $\hat{\theta}_{k-1}(t) < \frac{\gamma_1}{\gamma_2}\delta\boldsymbol{\omega}_k^{\mathrm{T}}(t)\tanh\left(\frac{\delta\boldsymbol{\omega}_k(t)}{\sigma}\right)$. Take $t = 0$ as an example, when γ_2 tends to zero, $\hat{\theta}_k(0)$ and $\boldsymbol{u}_k(0)$ will be too large as k tends to infinity if $\delta\boldsymbol{\omega}_k(0) \equiv C > 0$ holds. On the other hand, when γ_2 tends to one, the learning efficiency will be weakened. Therefore, there is a trade-off for the adjustment of γ_2. In addition, γ_1 faces the similar trade-off. Based on the above analysis, the control parameters are selected as $k_p = 2$, $k_d = 5$, $\gamma_1 = 10$, $\gamma_2 = 0.01$, and $\sigma = 0.0001$ according to the method proposed in Wie, Weiss, and Arapostathis (1989). In the simulation, the control frequency is 100 Hz, which is reasonable for the attitude control of spacecraft.

With the aforementioned simulation environment, the simulation results with the control law (10) and the parametric learning law (12) applied are presented in Figs. 1 and 2, which show that the attitude tracking performance is refined iteration by iteration. Fig. 1 shows the pointing trajectory of z axis for different iterations, and the tracking performance of $k = 10$ is obviously better than that of $k = 0$. Define the error Euler angle as $|\alpha_k(t)| = 2\arccos(\left[1 - \delta\boldsymbol{q}_k^{\mathrm{T}}(t)\delta\boldsymbol{q}_k(t)\right]^{\frac{1}{2}})$, which can be considered as the index of the attitude tracking performance. The trend of $\max_{t\in[0,T]}|\alpha_k(t)|$ and $\max_{t\in[0,T]}\|\delta\boldsymbol{\omega}_k(t)\|$ along the iteration axis are illustrated in Figs. 2(a) and 2(b), respectively, which clearly show that the attitude tracking errors converge to about 1 deg with the proposed controller and that the angular velocity errors converge to about 0.1 deg/s. It is worth emphasizing that in each iteration, initial state errors exist at $t = 0$ illustrated in Fig. 1, which cannot be handled with the conventional adaptive ILC in most works. In addition, the response of the control input torques for $k = 50$ is illustrated in Fig. 3(a), which indicates the smoothness of the control signals. Moreover, the boundedness property is verified from Fig. 2. It should be noted that the parameter estimate $\hat{\theta}_k(t)$ is not expected to converge to the true value because PE condition is not assured to be satisfied.

In order to demonstrate the effectiveness of the proposed method, we also present the controller and the learning law based on the sign function as

$$\boldsymbol{u}_k(t) = -k_p\delta\varepsilon_k(t)\delta\boldsymbol{q}_k(t) - k_d\delta\boldsymbol{\omega}_k(t) - \hat{\theta}_k(t)\,\mathrm{sgn}\,(\delta\boldsymbol{\omega}_k(t))$$

and

$$\hat{\theta}_k(t) = (1-\gamma_2)\,\hat{\theta}_{k-1}(t) + \gamma_1\delta\boldsymbol{\omega}_k^{\mathrm{T}}(t)\,\mathrm{sgn}\,(\delta\boldsymbol{\omega}_k(t))$$
$$\hat{\theta}_0(t) = 0, \quad \forall t \in [0, T],$$

simulation results of which are shown in Fig. 3. The evolution of the inputs illustrated in Fig. 3(b) shows the high-frequency

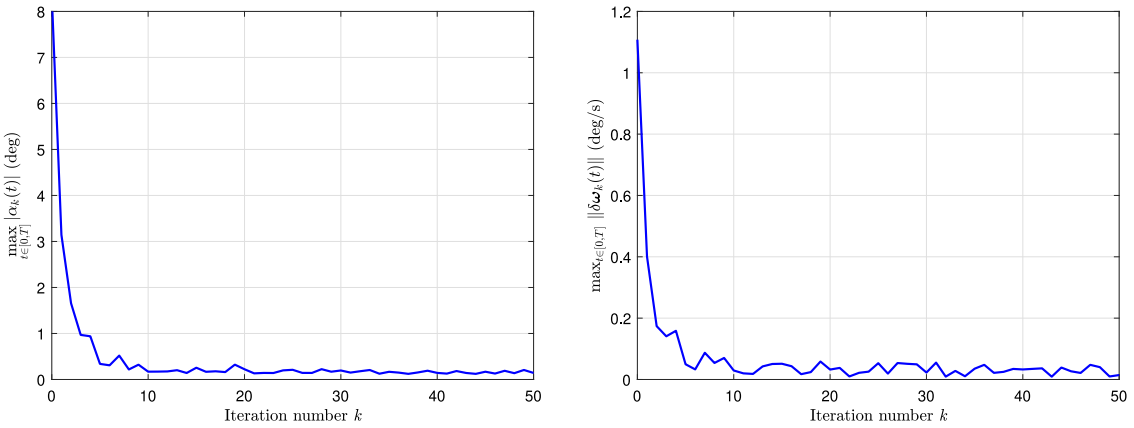

(a) $\max_{t\in[0,T]} |\alpha_k(t)|$ versus the number of iterations. (b) $\max_{t\in[0,T]} \|\delta\boldsymbol{\omega}_k(t)\|$ versus the number of iterations.

Fig. 2. Results when the hyperbolic tangent function is used.

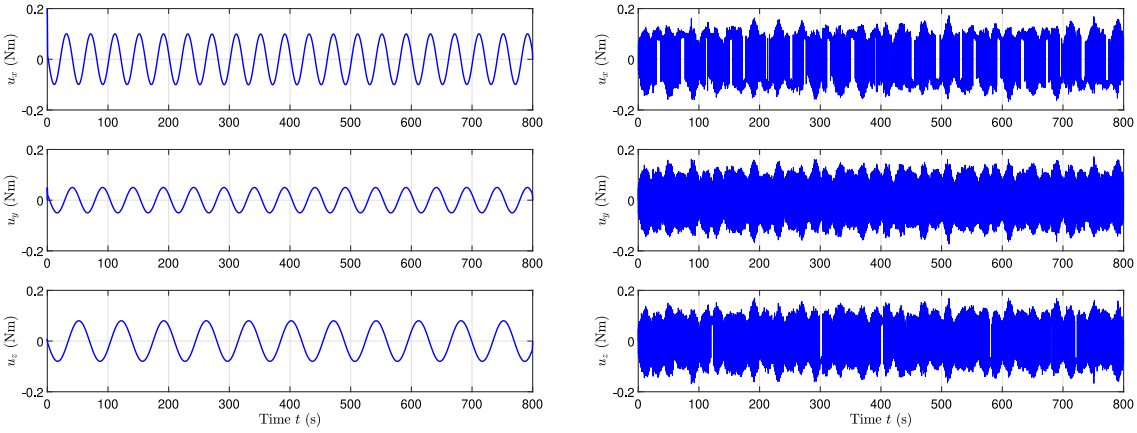

(a) With the proposed adaptive ILC (10) and (12). (b) With the adaptive ILC based on the sign function.

Fig. 3. The evolution of the control input torques for $k = 50$.

chattering phenomenon, which is avoided effectively in Fig. 3(a). Therefore, the proposed method including (10) and (12) is more practical for the attitude tracking.

6. Conclusions

To achieve robust periodic attitude tracking of spacecraft, we have developed a chattering-free adaptive iterative controller in combination with a new parametric learning law, which strengthens the robustness against initial state errors. Unlike conventional adaptive ILC with the sign function, the hyperbolic tangent function has been introduced in the proposed controller, which is effective to avoid the chattering phenomenon, however, results in non-negative definite problems. To handle this problem, a novel analytical method has been developed by integrating the CEF and CM methods. It has been shown that the iteration-varying initial state errors with unknown bounds, as well as unmodeled dynamics and external disturbances, can be treated effectively with the proposed control method. Simulation results have been illustrated to show the impressive control performance for the attitude tracking of uncertain spacecraft.

Acknowledgments

The authors would like to thank Dr. J. Zhang from Beihang University for his helpful discussions, and the associate editor and all reviewers for their valuable comments.

References

Abdessameud, A., Tayebi, A., & Polushin, I. G. (2012). Attitude synchronization of multiple rigid bodies with communication. *IEEE Transactions on Automatic Control*, *57*(9), 2405–2411.

Altın, B., & Barton, K. (2017). Exponential stability of nonlinear differential repetitive processes with applications to iterative learning control. *Automatica*, *81*, 369–376.

Bristow, D. A., Tharayil, M., & Alleyne, A. G. (2006). A survey of iterative learning control. *IEEE Control Systems Magazine*, *26*(3), 96–114.

Cavalcanti, J., Figueredo, L. F. C., & Ishihara, J. Y. (2018). Robust controller design for attitude dynamics subjected to time-delayed state measurements. *IEEE Transactions on Automatic Control*, *63*(7), 2191–2198.

Chien, C. J. (2008). A combined adaptive law for fuzzy iterative learning control of nonlinear systems with varying control tasks. *IEEE Transactions on Fuzzy Systems*, *16*(1), 40–51.

Cobb, M., Reed, J., Daniels, J., Siddiqui, A., Wu, M., Fathy, H., et al. (2022). Iterative learning-based path optimization with application to marine hydrokinetic energy systems. *IEEE Transactions on Control Systems Technology*, *30*(2), 639–653.

He, W., Meng, T., He, X., & Ge, S. S. (2018). Unified iterative learning control for flexible structures with input constraints. *Automatica*, *96*, 326–336.

Hu, Q., Xiao, B., Wang, D., & Poh, E. K. (2013). Attitude control of spacecraft with actuator uncertainty. *Journal of Guidance, Control, and Dynamics*, *36*(6), 1771–1776.

Hughes, P. C. (2004). *Spacecraft attitude dynamics*. Mineola, New York: Dover Publications.

Jin, X. (2017). Iterative learning control for non-repetitive trajectory tracking of robot manipulators with joint position constraints and actuator faults. *International Journal of Adaptive Control and Signal Processing*, *31*(6), 859–875.

Jin, X. (2019). Fault tolerant nonrepetitive trajectory tracking for mimo output constrained nonlinear systems using iterative learning control. *IEEE Transactions on Cybernetics*, *49*(8), 3180–3190.
Lang, X., & de Ruiter, A. (2022). Passivity-based iterative learning control for spacecraft attitude tracking on SO (3). *Journal of Guidance, Control, and Dynamics*, *45*(4), 748–754.
Lee, Y.-H., Rai, S., & Tsao, T.-C. (2022). Data-driven iterative learning control of nonlinear systems by adaptive model matching. *IEEE/ASME Transactions on Mechatronics*, *27*(6), 5626–5636.
Li, Q., Deng, Z., Zhang, K., & Wang, B. (2018). Precise attitude control of multirotary-joint solar-power satellite. *Journal of Guidance, Control, and Dynamics*, *41*(6), 1435–1442.
Li, X., Huang, D., Chu, B., & Xu, . J. X. (2016). Robust iterative learning control for systems with norm-bounded uncertainties. *International Journal of Robust and Nonlinear Control*, *26*(4), 697–718.
Li, Q., Wei, Y., Deng, Z., Wu, Z., & Jiang, J. (2021). Switched iterative learning attitude and structural control for solar power satellites. *Acta Astronautica*, *182*, 100–109.
Petersen, C. D., Leve, F., & Kolmanovsky, I. (2017). Model predictive control of an underactuated spacecraft with two reaction wheels. *Journal of Guidance, Control, and Dynamics*, *40*(2), 320–332.
Riel, T., Sinn, A., Schwaer, C., Ploner, M., & Schitter, G. (2019). Iterative trajectory learning for highly accurate optical satellite tracking systems. *Acta Astronautica*, *164*, 121–129.
Sammons, P. M., Hoelzle, D., & Barton, K. (2020). Time-scale transformed iterative learning control for a class of nonlinear systems with uncertain trial duration. *IEEE Transactions on Control Systems Technology*, *28*(5), 1972–1979.
Tayebi, A. (2004). Adaptive iterative learning control for robot manipulators. *Automatica*, *40*(7), 1195–1203.
Tayebi, A., Abdul, S., Zaremba, M. B., & Ye, Y. (2008). Robust iterative learning control design: Application to a robot manipulator. *IEEE/ASME Transactions on Mechatronics*, *13*(5), 608–613.
Wie, B., Weiss, H., & Arapostathis, A. (1989). Quaternion feedback regulator for spacecraft eigenaxis rotations. *Journal of Guidance, Control, and Dynamics*, *12*(3), 375–380.
Wu, B., Wang, D., & Poh, E. K. (2015). High precision satellite attitude tracking control via iterative learning control. *Journal of Guidance, Control, and Dynamics*, *38*(3), 528–534.
Xie, H., & Sun, M. (2009). Design of iterative learning controllers with finite-time dead-zone modification. *Control Theory & Applications*, *26*(11), 1225–1231.
Xing, X., & Liu, J. (2019). Modeling and robust adaptive iterative learning control of a vehicle-based flexible manipulator with uncertainties. *International Journal of Robust and Nonlinear Control*, *29*(8), 2385–2405.
Yang, S., Xu, J. X., Huang, D., & Tan, Y. (2015). Synchronization of heterogeneous multi-agent systems by adaptive iterative learning control. *Asian Journal of Control*, *17*(6), 2091–2104.
Yin, C., Xu, J. X., & Hou, Z. (2011). An ILC scheme for a class of nonlinear continuous-time systems with time-iteration-varying parameters subject to second-order internal model. *Asian Journal of Control*, *13*(1), 126–135.
Zhang, J., & Meng, D. (2021). Iterative rectifying methods for nonrepetitive continuous-time learning control systems. *IEEE Transactions on Cybernetics*, *53*(1), 338–351.
Zhang, J., & Meng, D. (2022). Improving tracking accuracy for repetitive learning systems by high-order extended state observers. *IEEE Transactions on Neural Networks and Learning Systems*, http://dx.doi.org/10.1109/TNNLS.2022.3166797, Early access.
Zhang, F., Meng, D., & Li, X. (2022). Robust adaptive learning for attitude control of rigid bodies with initial alignment errors. *Automatica*, *137*, Article 110024.
Zhao, Q., & Duan, G. (2021). Concurrent learning adaptive finite-time control for spacecraft with inertia parameter identification under external disturbance. *IEEE Transactions on Aerospace and Electronic Systems*, *57*(6), 3691–3704.

Fan Zhang received the B.Eng. degree in detection, guidance and control technology and the M.Eng. degree in navigation, guidance and control from the School of Astronautics, Northwestern Polytechnical University (NWPU), Xi'an, China, in 2015 and 2018, respectively. He is currently pursuing the Ph.D. degree with the School of Automation Science and Electrical Engineering, Beihang University (BUAA), Beijing, China. His current research interests include iterative learning control, networked control systems, and space flight dynamics and control.

Deyuan Meng received the B.S. degree in mathematics and applied mathematics from Ocean University of China (OUC), Qingdao, China, in June 2005, and the Ph.D. degree in control theory and control engineering from Beihang University (BUAA), Beijing, China, in July 2010. From November 2012 to November 2013, he was a Visiting Scholar with the Department of Electrical Engineering and Computer Science, Colorado School of Mines, Golden, CO, USA. He is currently a Full Professor with the Seventh Research Division and the School of Automation Science and Electrical Engineering, Beihang University (BUAA). His current research interests include iterative learning control, data-based control, and multi-agent systems.

Xuefang Li received the B.Sc. and M.Sc. degrees with a major of pure mathematics from the Mathematical College, Sichuan University, Chengdu, China, in 2009 and 2012, respectively. She attended the Department of Electrical and Computer Engineering (ECE), National University of Singapore (NUS), Singapore, in 2012, where she received the Ph.D. degree with a major in control engineering in 2016. From September 2016 to August 2019, she was a Research Associate with the Department of Electrical and Electronic Engineering (EEE), Imperial College London, London, U.K. She is currently an Associate Professor with the School of Intelligent Systems Engineering, Sun Yat-Sen University, Guangzhou, China. Her research interests include advanced control theory, robotics, and intelligent vehicles. She is a member of the IEEE CSS and IEEE IES.